Development of a Corrugated Test Specimen for Composite Materials Energy Absorption

PAOLO FERABOLI*
Department of Aeronautics and Astronautics
University of Washington, Seattle, WA 98195–2400, USA

ABSTRACT: One of the key factors preventing the widespread adoption of composites in primary crash structures is the absence of specialized test methods for the characterization of specific energy absorption (SEA). Aside from thin-walled tubular specimens, a limited number of attempts have been made at using a plate specimen, which is easier to manufacture but requires complex anti-buckling fixtures. A new method, featuring a corrugated plate, which can be easily manufactured and is self-stabilizing and hence does not require a dedicated test fixture, is suggested here. A systematic investigation is performed to validate the possibility of using such specimen to screen candidate material systems and laminate designs, with the specific goal of isolating the sensitivity of the method to intrinsic specimen parameters.

KEY WORDS: crashworthiness, specific energy absorption, test standard.

INTRODUCTION

THE FOUR NECESSARY conditions for survival during a vehicle collision are maintaining sufficient occupant space, providing adequate occupant restraint, employing energy-absorbing devices, and allowing for a safe post-crash egress from the craft [1]. Specifically, the energy-absorbing components, primary vehicle structure and secondary systems must all be designed to work together to absorb the vehicle kinetic energy and slow the occupants to rest without injurious loading. Vehicle impact events involve the simultaneous structural response of multiple components, and often the energy-absorbing devices experience combined loading, resulting from axial crushing and bending. However, the complexity of these events is such that often these processes need to be approached individually, and usually the energy-absorbing components are designed to dissipate energy under controlled collapse in simpler loading configurations. In general, while the total energy dissipated during a crash depends on the overall vehicle system deformation, the crash-oriented design of the individual structural subcomponents of simple geometry

*E-mail: feraboli@aa.washington.edu
Figures 1, 4–6, 13–21, 23 and 26 appear in color online: http://jcm.sagepub.com

0021-9983/08/03 0229–28 $10.00/0 DOI: 10.1177/0021998307086202

can provide a great increase in structural crashworthiness and survivability, with an acceptable increase in overall vehicle cost. For this reason, structural elements that provide energy absorption have received special attention in the literature [2–6].

Energy absorbers can be found in the front end of all modern passenger cars, in the form of collapsible tubular rails [4,5], or in the keel of modern aircraft (Figure 1) as collapsible floor supports [6–10]. These elements have been traditionally made of steel or aluminum, which absorb energy through controlled collapse by folding and hinging, involving extensive local plastic deformation [2]. However, the introduction of composites in the primary structure of modern air- and ground-vehicles presents special problems for the designer dealing with occupant safety and crashworthiness. The energy-absorbing behavior of composites is not easily predicted due to the complexity of the failure mechanisms that can occur within the material. Composite structures fail through a combination of fracture mechanisms. These involve a complex series of fiber fracture, matrix cracking, fiber-matrix debonding, and interlaminar damage (delamination) mechanisms. The brittle failure modes of many polymeric composite materials can make the design of energy-absorbing crushable structures difficult. Furthermore, the overall response is highly dependent on a number of parameters, including the geometry of the structure, material system, lay-up, and impact velocity. Thus, extensive substructure testing is usually required within a building block approach to the design of crashworthy structures, in order to verify that a proposed configuration will actually perform as intended.

Recent studies [4,10] identified the key factors preventing the introduction of composites in primary crash-resistant structures in aircraft and automotive as the absence of:

- available design guidelines,
- accurate and inexpensive simulation tools,
- specialized test methods for the characterization of energy-absorption,
- accessible and adequate composite material property database.

Only a coordinated cross-organizational effort can lead to substantial advances in all these fronts through systematic investigations of current practices and

Figure 1. *Composite-intensive study of energy-absorbing subfloor of commuter aircraft [8].*

suggested improvements. Such efforts are for example being made the Crashworthiness Working Group of the CMH-17 (Composite Materials Handbook, formerly known as MIL-HDBK-17), which comprises representatives from the aerospace and automotive industry, academia, and government laboratories and operates in parallel with ASTM Committee D-30 on Composite Materials. Similarly, the Energy Management Working Group of the Automotive Composites Consortium (ACC), which comprises members of the three largest US automotive manufacturers and of the Department of Energy, has dedicated over two decades to advancing the understanding and confidence in composite crash structures.

When analyzing the energy absorption behavior of a structure, a few key definitions are required:

- Peak Force, the maximum point on the Force-stroke diagram.
- Average Crush Force. Also referred to as Sustained Crush Force, is the displacement-average value of the force history.
- Crush Load Efficiency. Ratio between the Peak and the Average Crush Force, ideally equal to unity.
- Stroke. Also referred to as crush or displacement, is the length of structure/material being sacrificed during crushing.
- Crush Initiator. Also known as trigger mechanism, a design feature that facilitates the progressive collapse of the structure, thus reducing spikes in the load–stroke diagram. Without a crush initiator, composite structures have a tendency to reach unacceptably high values of peak force, and can fail in an unpredictable and sometimes unstable manner. Triggers can manifest in the form of plug-type insert, chamfer, or embedded ply drop.
- Energy Absorbed (EA). Total area under the Force–Stroke diagram.
- Specific Energy Absorption (SEA). The energy absorbed per unit mass of crushed structure.

The ability of a material to dissipate energy can then be expressed in terms of SEA, which has units of J/g, and indicates a number, which for composites is usually comprised between 15 and 80 J/g. Setting the mass of structure that undergoes crushing as the product of stroke l, cross-sectional area A, and density ρ:

$$SEA = \frac{EA}{\rho A l}. \tag{1}$$

The EA can be calculated as the total area under the force–stroke diagram:

$$EA = \int F dl \tag{2}$$

where F is the instantaneous crush force. The average crush force F_{avg} is:

$$F_{avg} = \frac{\int F\, dl}{l} = \frac{EA}{l}. \tag{3}$$

REVIEW OF EXISTING WORK

Only a selected number of attempts have been made at developing a coupon-sized test method to determine the SEA of composite materials. The vast majority of the work in the area of crashworthiness energy absorption has focused on thin-wall tubular specimens [2–6]. A wide range of experimental set-ups have been used to establish a basic understanding of the influence of failure mechanisms, constituent fiber and matrix materials, and specimen geometry on the measured SEA. It has been shown that it is very important to employ a trigger mechanism to facilitate crush initiation [2], but there is not yet an agreement on what type of trigger should be employed [4,8]. It has also been shown that the sustained crush force is highly dependent on the shape of the tube undergoing crush testing. However, while the ACC employs a square specimen, the rotorcraft community, as well as racecar manufacturers, employs circular specimens. It has also been demonstrated that there can be a two-fold decrease in SEA between quasi-static and dynamic crush tests [4], while other authors have reported an increase over quasi-static results [2]. Yet, virtually every manufacturer uses different specimen geometries, set-ups, and loading rates to assess the energy absorption of their designs. Comparisons across different materials and stacking sequences are still very limited and only in a few occasions they have been performed systematically. The lack of an agreed upon test method makes the comparison of test results and research findings across the literature virtually impossible.

As mentioned, limited work has been done with test geometries other than tubes, and it evolved in two directions. The first approach features simple specimens, such as flat plates with or without built-in crush initiators, and very complex and costly anti-buckling support fixtures. The second approach features self-supporting specimen geometries, which require dedicated molding tool for manufacturing, but do not require the use of specific test fixtures. The Army Research Laboratories (ARL) in conjunction with Virginia Tech performed pioneering work done in the early 1990s at NASA Langley Research Center. The method proposed was considered by several laboratories [11,12] but was eventually abandoned due to some limitations. Over the years however, the NASA/ARL coupon idea was further developed, independently and in very different ways, by an engineering services firm based in the UK, Engenuity Ltd, which currently uses it commercially to provide SEA data to several motorsport and automotive companies, and by the US Department of Energy (DoE) at Oak Ridge National Laboratory. Even less effort has been aimed at developing self-supporting specimens, and the German Aerospace Research Center (DLR) is the only one that has developed and currently employs one of semi-circular shape [11]. The following sections will review in detail the advantages and shortcomings of each of the above test methods in order to introduce the proposed test method.

Flat Specimens with Support Fixtures

The ARL group proposed a test method featuring a flat plate rectangular specimen (Figure 2, left) and a dedicated test fixture designed to provide buckling stability during crushing [13–15]. Lateral support to the specimen is provided through knife-edges, which fit into a set of four inner vertical posts. Two types of trigger mechanisms, the so-called ‘steeple’ and the ‘notch’ (a staggered, transverse machined profile) were both employed with success. However, the steeple trigger had a tendency to generate a double peak in the

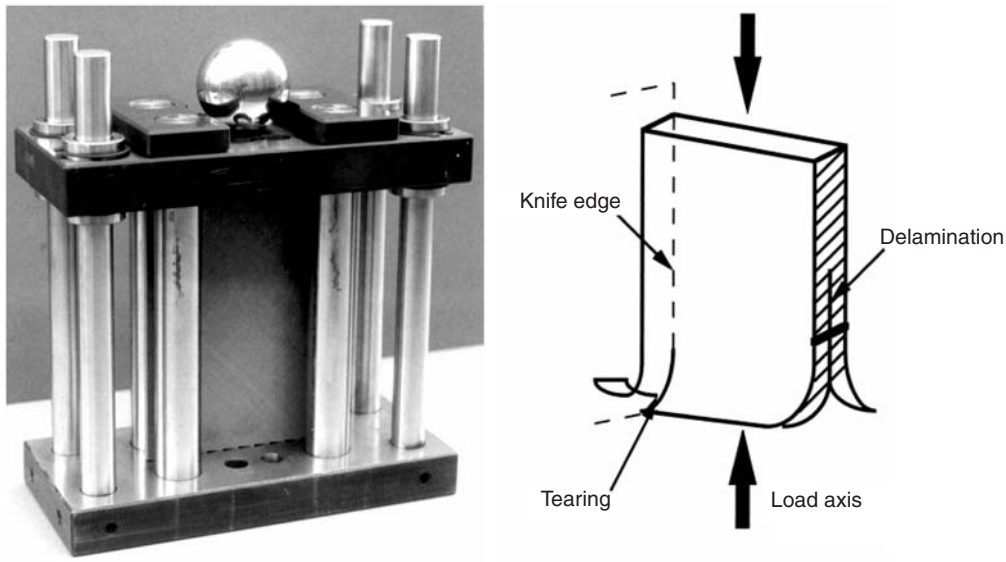

Figure 2. *(Left) Test fixture and specimen developed by the ARL [13–15]. (Right) Undesirable characteristic of this set-up is the tearing at the supports, which produces unrealistic SEA values [16,17].*

initial portion of the load–stroke diagram, possibly due to the formation of a long delamination along the specimen length. The 45-degree chamfered trigger, commonly used in tubular specimens, was not employed because apparently it was unable to initiate crushing. In conclusion to their study, the authors suggested a list of changes that could be implemented to improve the current design, including making the knife-supports adjustable in width and depth, in order to easily accommodate specimens of varying thickness and width, and using a different trigger mechanism, such as a J-trigger, possibly in the form of a molded-in curl at the end of the plate. However, the greatest limitation of this fixture was that the knife-edge supports promote local tearing of the plate and fronds (Figure 2, right). This failure mechanism is responsible for vast amounts of energy absorption, comparable to the amounts dissipated in frond formation, and thus leads to unrealistic SEA values. Although the fixture yielded force-stroke traces that closely resembled those of tubular specimens, the SEA measurements obtained with this method did not compare well with others previously obtained [3] by testing thin-wall tubular specimens of the same material systems and laminate designs. It is likely that the two specimens fail by somewhat different mechanisms. In particular, the off-axis fibers provide hoop constraint to the tubular shape, thus suppressing outward brooming of the longitudinal fibers, and facilitating fiber fragmentation. On the other hand, for flat shapes, no such constraint is available, and it leads to the creation of a strong interlaminar separation front (similar to a traveling wedge test for adhesive joints). It can be summarized that for flat plate specimens, delamination suppression is indeed crucial to maintain high levels of energy absorption, however the material cannot be over-constrained and it has to be left free to follow its natural failure mode.

Investigators at the University of London recently revisited the ARL fixture and modified it to account for variable specimen width and thickness by introducing adjustable knife-edge supports [16,17]. They also focused on a 45-degree steeple trigger only, which

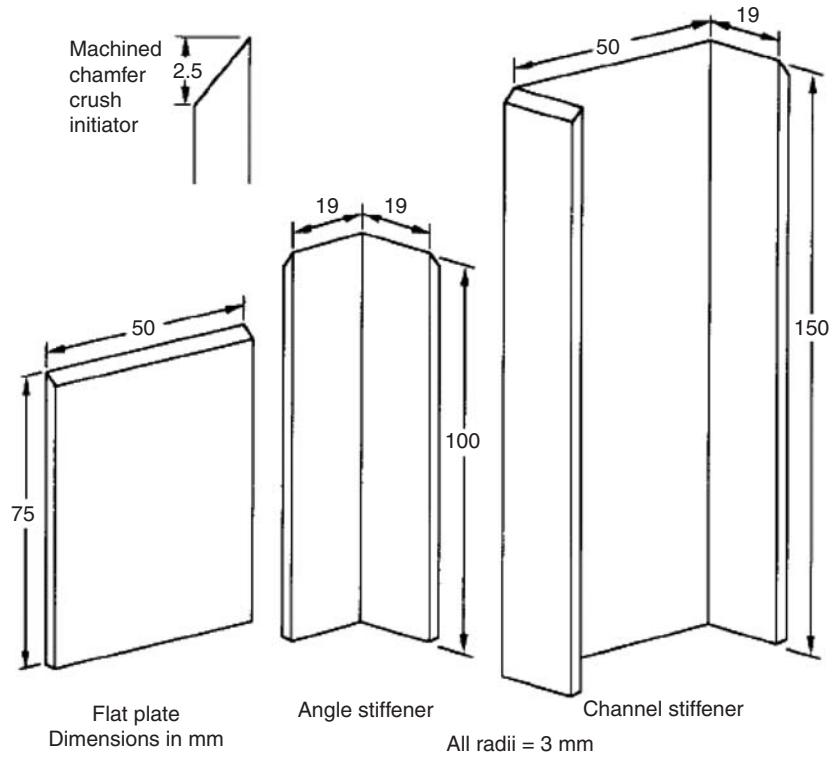

Figure 3. *Systematic comparison of specimen geometry on the measured SEA [12].*

Table 1. Referring to Figure 3, results of the systematic comparison of specimen geometry on the measured SEA in J/g for two stacking sequences [12].

Lay-up	Flat	Angle	C-channel
$[45]_{10}$	89	54	68
$[45_2/O_2/45_2]_s$	96	67	83

confirmed to promote a double-stage initial collapse. However, the inherent limitations of the tearing at the supports of the ARL fixture were not resolved.

In the effort to understand the validity of the proposed flat plate specimen, Bolukbasi and Laanen [12] conducted a systematic comparison of three structural configurations. Flat plates, angle sections, and C-channels manufactured with identical materials, lay-ups, and crush initiators were crushed under the same quasi-static conditions (Figure 3). Although the number of specimens tested was limited, as the selection of laminate lay-ups, it was confirmed that the flat plates tested with the ARL fixture yielded higher SEA measurements than any of the self-supporting specimens (Table 1).

Building on the ARL concept, Engenuity [18] developed a rig that provides buckling stability by fully constraining lateral and out-of plane movement of the coupon, while at

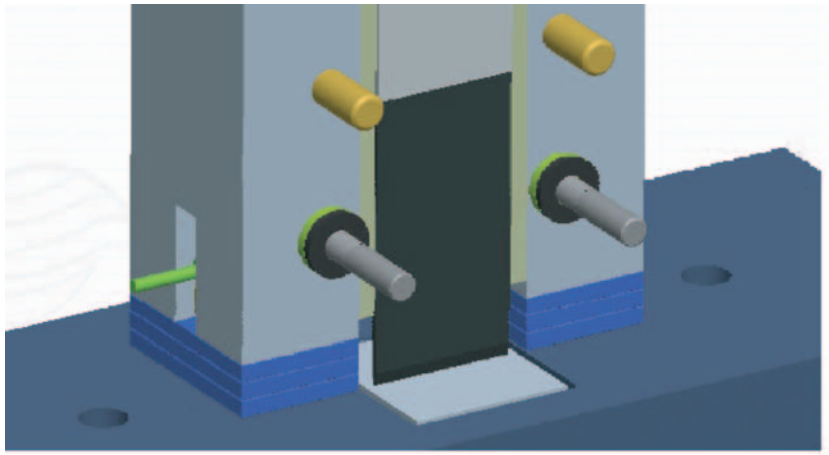

Figure 4. *Test fixture and specimen (with relative trigger mechanism) developed by Engenuity.*

the same time enables it to deform freely in the proximity of the crush front. The specimen is a flat rectangular plate, and features a trigger with saw-tooth (jagged) edge. Such trigger is planar, as the notched trigger used by ARL, since its profile does not vary through the specimen's thickness, unlike the chamfer and steeple triggers. The fixture features Delrin supports to reduce the friction on the surfaces contacting the specimen, and can accommodate specimens of varying thickness (Figure 4). The greatest difference with respect to the ARL fixture is that the specimen is here allowed to deform freely in proximity of the crush front. This is achieved by leaving an unsupported distance between the specimen supports and the base-plate. This distance, which Engenuity refers to as 'spacer height', allows the material to crush in a more natural way. However, the unsupported height affects the degree of delamination suppression that can be guaranteed. This in turn means that material systems with high interlaminar fracture toughness, hence resistance to delamination propagation, can achieve high values of SEA even in the presence of large unsupported heights. On the other hand, more brittle systems offer poor crush performance, and fail by delamination propagation on the interlaminar front [18]. To the limit, all materials will absorb large amounts of energy if the spacer height is zero, as in the ARL fixture. This effectively dictates a strong dependence of SEA measurement on unsupported height, and Engenuity varies this spacer height in the range 5–30 mm for every material characterization operation.

The Department of Energy (DoE) developed a test method [19,20] with which to reproduce and isolate the splaying failure mode typical of composite thin-wall tubes, which occurs through frond formation. The specimen consists of a flat, slender rectangular plate, and requires no machining. Crushing is initiated by means of a contoured contact profile rather than a machined or molded-in trigger, and the frond splaying response is obtained through a J-shaped base-plate in a fashion similar to plug-type initiators used by the ACC [5]. Buckling support is provided in the form of a series of frictionless roller supports (Figure 5). The fixture is characterized the interchangeable contact profile, where crush occurs, and an additional contact constraint in the form of an adjustable roller. The degree of constraint provided by the roller near the crush front is key in achieving favorable crush characteristics, and stable crushing occurs only under certain degree of constraint.

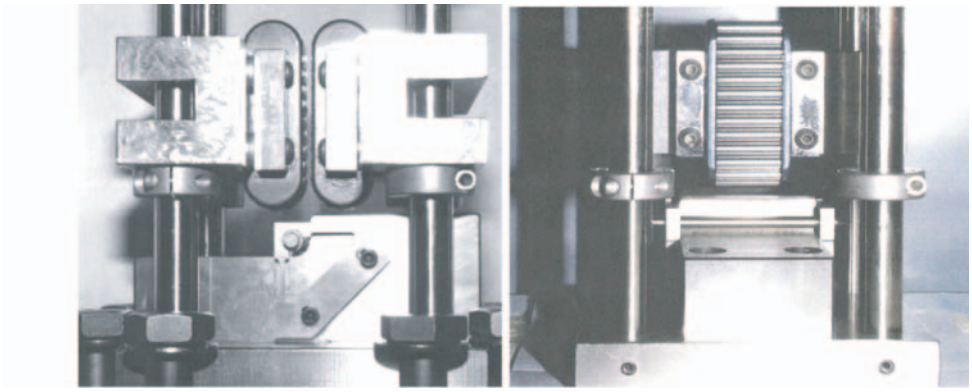

Figure 5. *Front and side views of the test fixture developed by the DoE [19,20].*

The curvature of the contact profile bears also a great effect on the SEA, as increasing profile radius causes a decrease in SEA, likely due to the more flexural rather than compression deformation experienced by the specimen tip. SEA measurements with the proposed specimen are therefore very sensitive to these two parameters, and extensive calibration would be required to develop a better understanding.

Brimhall [21], in conjunction with the ACC and DoE, employed a somewhat similar plate specimen and fixture to further characterize the energy absorbed by the fronds in friction at contact with the crush surfaces. Quasi-static and dynamic friction coefficients were identified to be responsible, in varying amounts, for large portions of the energy absorbed on crushing. Furthermore, the study suggested that only a small portion of the energy is absorbed by fiber tearing, while most of it is absorbed in frond formation and friction against the base.

Contoured Self-Supporting Specimens

In order to compare the SEA of different composite systems and laminate designs, Johnson and Kohlgruber of the German Aerospace Agency (DLR) [11] developed a tube-segment specimen, which is easy to fabricate (does not require an internal mandrel) and gives reproducible crush failures under quasi-static and dynamic axial loads. The end-lips, or flanges, provide additional stability to the semicircular shell, but the specimen is also mounted with adhesive in a contoured aluminum base (Figure 6). A 45-degree chamfer is machined on the other end to initiate crushing. Although it is not clear how the specimen came to be designed to the final proposed geometry, it was shown that the specimen yields desirable and stable crushing force-stroke traces. Current literature is however limited and further work is needed to show how the measured SEA compares with that of other geometries, such as tubular specimens.

The same semicircular specimen of the DLR has been successfully used by Dormegnie et al. of the French Aerospace Agency (ONERA) under the name of Omega specimen [22]. The DLR-sized specimen is scaled geometrically up to four times to explore laminate stacking sequence scaling effects. Although stable crushing characteristics can be observed from the partial force–displacement curves, the experimental investigation does not discuss in detail the influence of specimen geometry on the measured force.

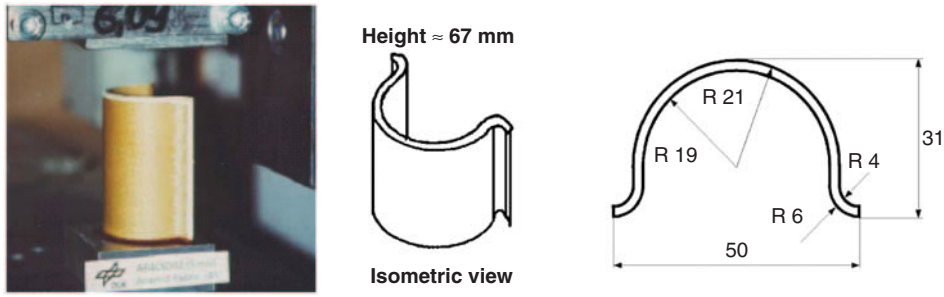

Figure 6. *Semi-circular self-stabilizing specimen developed by DLR [11], all dimensions in mm.*

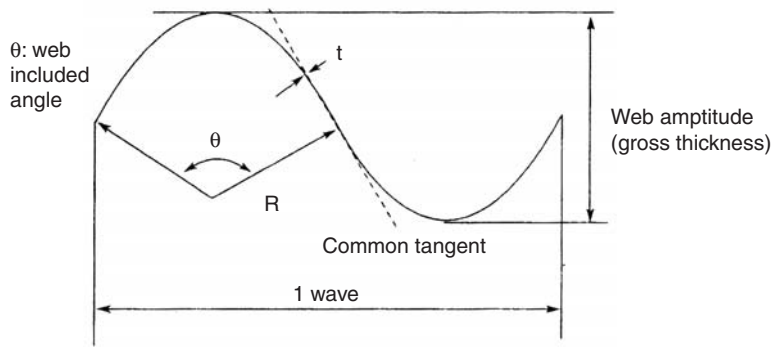

Figure 7. *Sine web terminology used in Ref [24].*

An attempt was also made by Fleming and Nicot [23] to develop a cruciform specimen, which can be seen as the intersection of four individual flat ARL specimens. Its self-supporting nature made it appealing because it did not require a dedicated test fixture. However, effective triggering of progressive crushing was difficult, as well as machining of the trigger itself, and manufacturing of the specimen required a complex decomposable mold. For these reasons the specimen was not further pursued.

Hanagud et al. [24], under contract of the ARL, conducted a systematic investigation of the crushing performance of sine webs (also referred to as corrugated webs). The specimen used in the investigation is a sine web 89 mm (3.5 in) high, comprised of tangentially joined circular arc segments (Figure 7). The arc radius is kept fixed at 9.5 mm (0.375 in) but the included angle is varied between 0, 60, 90, 120, 150, and 180 degrees. To the extreme, a 0-degree angle corresponds to a flat specimen, while a 180-degree angle corresponds to a full semicircle. Specimen width is varied between 1, 2, and 3 waves (or half-periods). Although not explicitly mentioned, it seems that the width of one wave varies between 9.5 mm (0.375 in) for the 0-degrees specimen, to 19 mm (0.75 in) for the 180 degrees. Three types of triggers are employed, namely the chamfer, notch, and ply drop, consistently with the ARL designation. The length of the trigger is also varied between 3.2 mm (0.125 in) and 12.7 mm (0.5 in). Only one material system is used and it is of relatively brittle nature. Tests are performed only at a quasi-static rate of 2 mm/min (0.08 in/min) up to approximately 50% stroke. All energy absorption data is reduced to Specific Sustained Crush Stress (SSCS), which is the same as SEA.

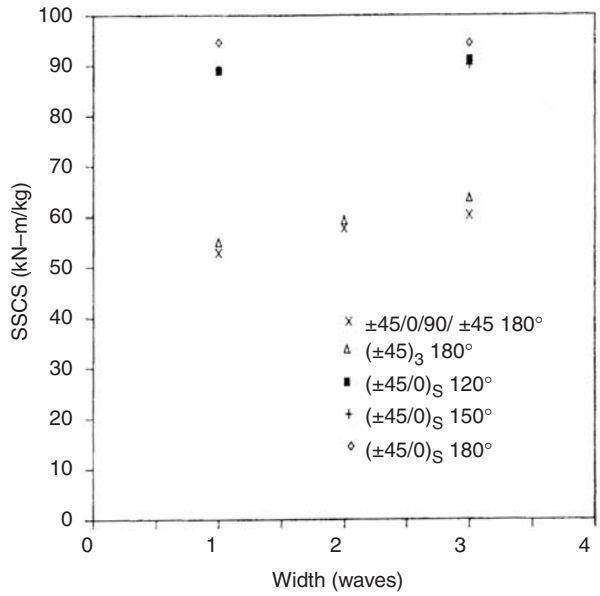

Figure 8. *Influence of number of wave repetitions (hence total width) for various lay-ups and wave amplitudes [24].*

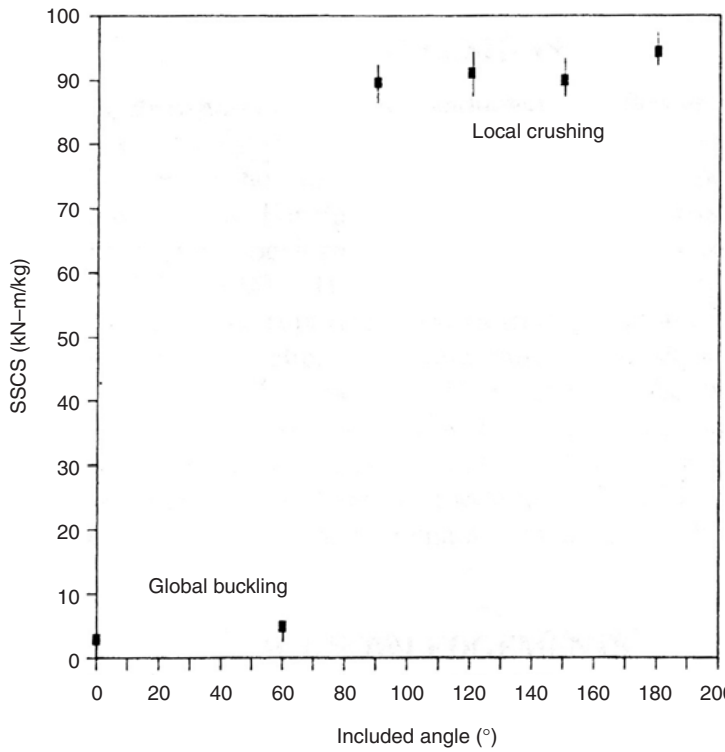

Figure 9. *Influence of the included angle (degree of corrugation) on energy absorbed [24].*

Among the several findings of the study, it is shown that all three trigger mechanisms lead to the same SSCS values, which suggests that the sine web specimen is robust to initiator design. However, increasing trigger length leads to progressively lower values of SSCS, which leads the authors to explore future work. Another observation shows that for the material system tested, the influence of specimen width on SSCS, as measured by the number of wave repetitions, ranges from zero to a few percent according to the lay-up (Figure 8). A fundamental observation is that varying the value of the included angle has minor effects in the range 90–180 degrees, but that for lower values (60 and 0 degrees) the energy absorption drops significantly due the loss of stability (Figure 9). It is therefore fundamental to maintain a sufficient degree of corrugation for the specimen in order to ensure the onset of progressive crushing over macroscopic buckling.

Lastly, it is shown that for a limited set of lay-ups and for the material tested, SSCS measurements obtained with the sinusoidal specimen are equal to those obtained with tubular specimens through other ARL-sponsored programs [14]. Overall, from this study as well as other observation on the crushing response of corrugated web structures it can be said that they offer a good degree of robustness to geometric shape parameters, while requiring minimal amount of fixturing and manufacturing costs.

PROPOSED METHODOLOGY

Experimental Set-up and Specimen Fabrication

Reviewing the proposed colupon-level test methodologies [25], the approaches featuring a simple specimen shape and a complex test fixture appear to be characterized by several variables that need to be carefully understood. The dependence of SEA measurements on intrinsic test set-up parameters (such as unsupported height, degree of constraint, trigger type, and contact profile shape) makes this type of test impractical for standardization. On the other hand, the approach that pursues a dedicated specimen shape but a very general test set-up seems to allow for easier generalization of results. Although intrinsic specimen shape parameters (such as aspect ratio) need to be studied systematically, it seems more likely that they will have a less direct impact on the measurement of the SEA. The popularity of thin-walled tubular specimens can be also attributed to their simple and versatile set-up.

The research presented here focuses on the development of a corrugated plate specimen, which requires the use of a dedicated molding tool, but on the other hand does not require the use of a specialized test fixture. Its self-supporting nature is such that the specimen can deform freely in proximity of the crush front, yet its three-dimensional geometry is such that it can capture the majority of failure modes observed for tubular specimens. All but hoop-fiber tension failure of off-axis plies, which can be seen only in tubular specimens but has been shown to absorb relatively low amounts of energy [21], can be reproduced in the corrugated specimen.

Corrugated webs have been used for several energy-absorbing applications in fixed wing, rotorcraft, and racecar structures [7,8,10,26,27] because of their favorable crushing response (Figure 1). However, no systematic study has been performed or published attempting to understand the influence on the measured SEA of the corrugation characteristics, such as shape, amplitude, and number of half-period repetitions. This paper provides the foundation for the development of a test standard based on a

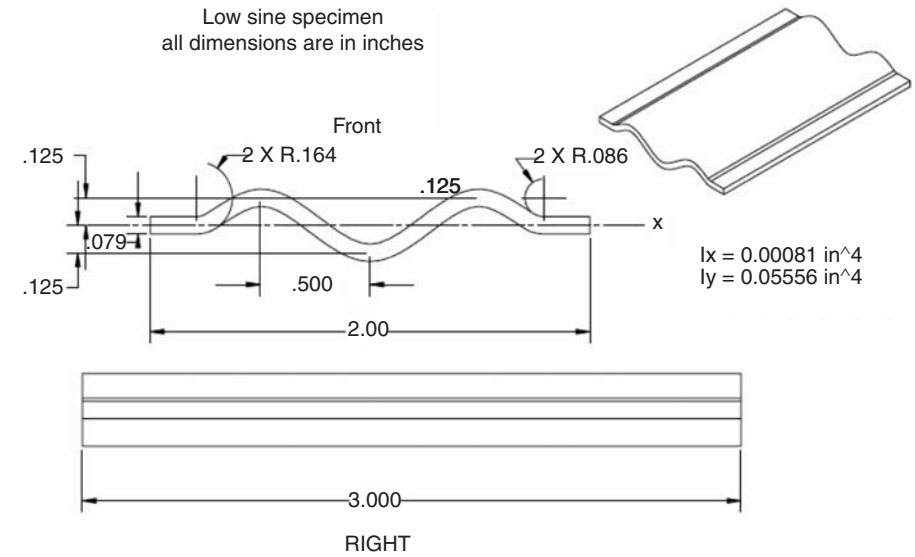

Figure 10. *Detailed geometry of low sine specimen.*

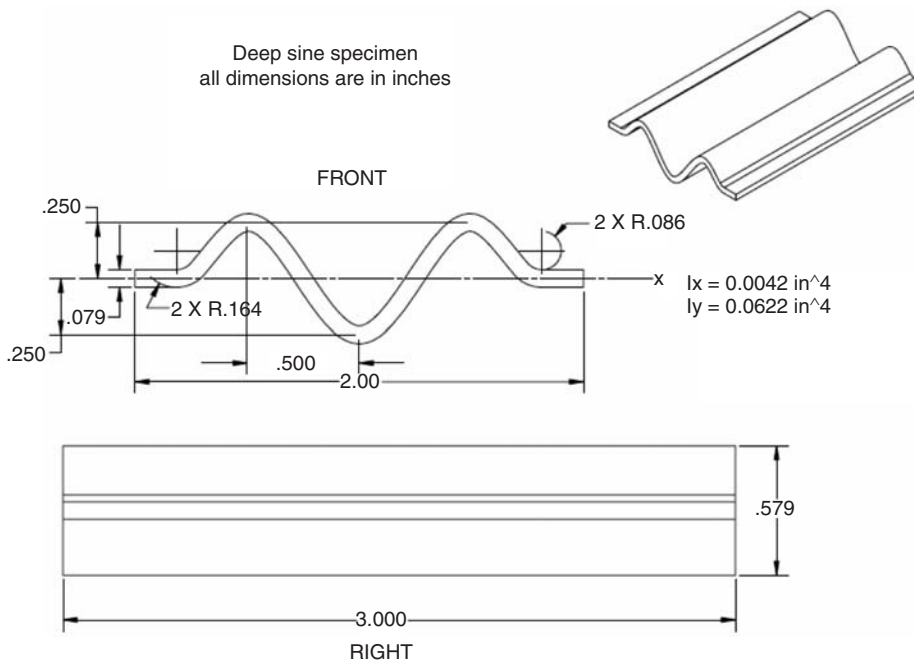

Figure 11. *Detailed geometry of high sine specimen.*

corrugated web geometry through a parametric investigation of several intrinsic as well as explicit variables. Three different corrugated shapes are investigated in the attempt to understand how the degree and shape of corrugation affect both stability and crush performance of the section. The specimen denoted 'low sine' features a sinusoidal segment,

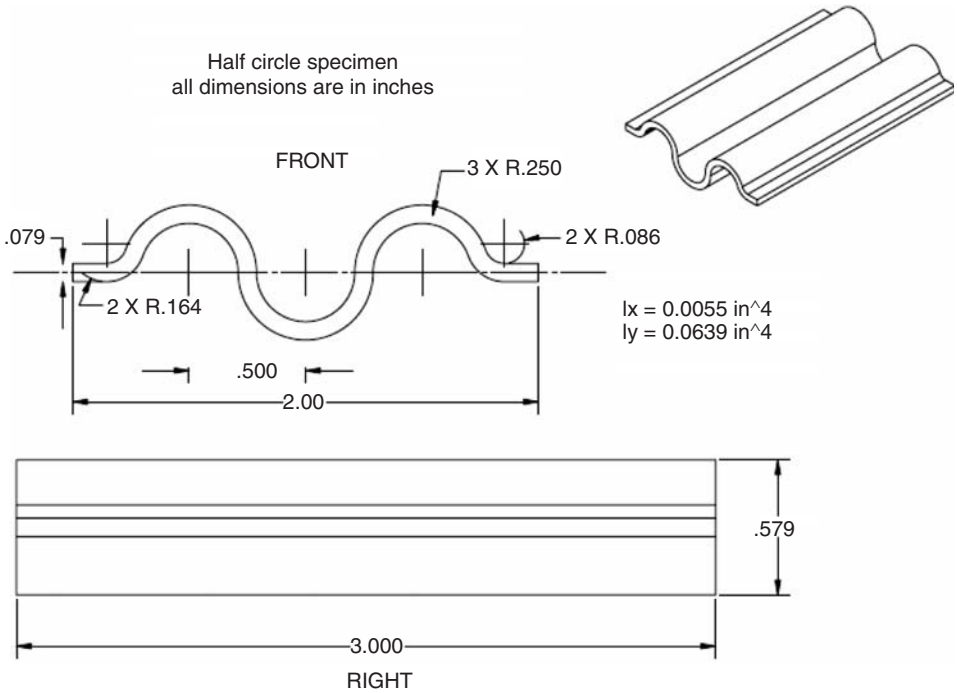

Figure 12. *Detailed geometry of semi-circle specimen.*

of amplitude 3.2 mm (0.125 in.), repeated three times at alternating sides with respect to the midplane (see Figure 10). The specimen denoted as 'high sine' features a sinusoidal segment, of amplitude 6.4 mm (0.25 in.), repeated three times at alternating sides with respect to the midplane (see Figure 11). The specimen denoted as 'semicircle' features a semicircular segment, of radius 6.4 mm (0.25 in.), repeated three times at alternating sides with respect to the midplane (see Figure 12). Each repetition of the unit corrugation about the midplane is a half-period. All three segments have end-lips, or straight edges, of material on each side of the corrugation for additional stability. Since buckling considerations govern the design of the specimen, it useful to note that if we use the moment of inertia for the low sine specimen as the reference (unity), the moments of inertia for the high sine and for the semicircle specimens are 3.83 and 4.79 times respectively.

Specimens are manufactured by press-molding through a set of aluminum matching tools (Figure 13). The lower mold can however be used for open-molding processes as well, such as vacuum bagging for autoclave cure. The molds outer dimensions are 305 mm × 305 mm (12 in. × 12 in.) and feature an effective (machined) area that yields specimen panels 203 mm × 203 mm (8 in. × 8 in.). For a given material system and lay-up, each molding cycle yields a specimen panel from which six coupons can be obtained, two for each of the three corrugated shapes. Each coupon is 76.2 mm long (3 in.) and 50.80 mm wide (2 in.) from end-lip to end-lip. Detailed dimensions are shown in Figures 8–10. The molds feature alignment pins for accurate positioning. Prior to lay-up, a thin layer of mold release coating is brushed onto the mold surfaces to facilitate release of the specimens. Release film was used in earlier studies but proved to be difficult to use, as the plies tended to slide over it during lay-up.

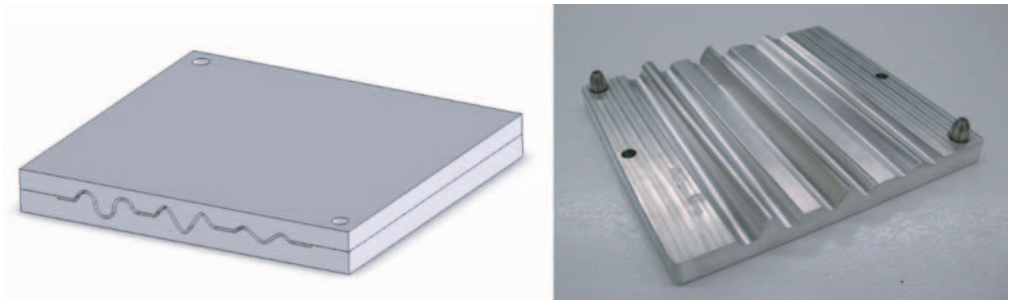

Figure 13. *Molding tool.*

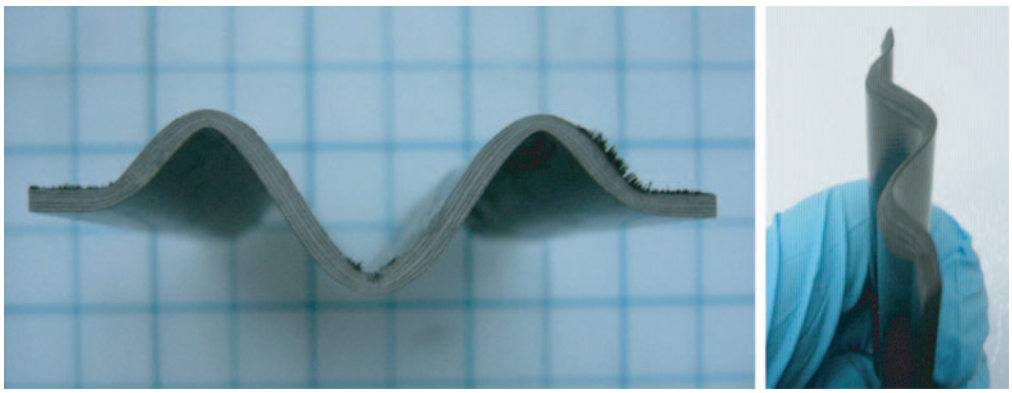

Figure 14. *High sine specimen with chamfered end.*

After cure, specimens are machined from the as-molded panel, and are further chamfered with a single-sided 45-degree chamfer (Figure 14) such as the one used in tubular specimens and in the DLR specimen [11]. One specimen was tested without chamfer in the early stages of the research and showed crush load efficiency of 2.5, which is unacceptably high. However, the sustained crush load was not different from the chamfered specimens tested later. No other types of trigger mechanisms are employed in this study, although future work may consider the use of internal ply-drops to initiate stable crush.

Specimens are tested in vertical configuration, resting on a polished hardened steel surface (Figure 15). The crushing plate is free to slide along four vertical posts, which use roller bearings for alignment and reduced friction. A self-aligning sphere is used to introduce the load from the test frame onto the crushing plate. For each configuration at least two specimens are tested, which are not sufficient to build a statistical database but can provide insight in the validity of the proposed method.

Design of Experiment

A test method such as the one proposed here could be used to determine the SEA values to be used in the sizing of a vehicle's energy absorbers, but also to screen

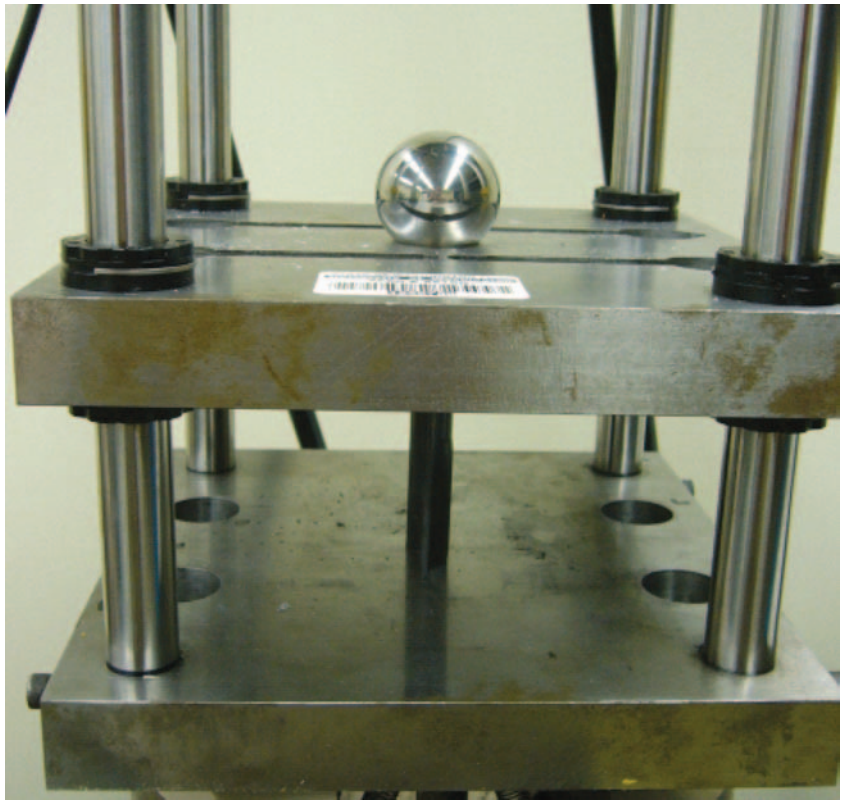

Figure 15. *Specimen ready for testing in the test fixture.*

Table 2. Design of experiment (DOE) summarizes the test parameters investigated.

DOE	1	2	3
Shape	High Sine	Low Sine	Semi-circle
Lay-up	[0/90]3s	[±45]3s	[0/±45]2s
Material	Regular	Tough	–
Shape	2 Sines	3 Sines	–
Cure	Regular	Overcured	–
Speed	0.2	2	60

material systems, compare laminate designs, and characterize strain rate sensitivity. It is therefore necessary to verify its sensitivity to both intrinsic and test parameters. A parametric investigation was developed to isolate and compare the effects of corrugation shape, laminate lay-up, material system, number of corrugations, and manufacturing inaccuracies (Table 2). This sensitivity study is designed to verify the ability of the proposed corrugated specimens to capture differences in measured SEA due to different specimen characteristics.

As discussed earlier, three different corrugated web shapes are selected for investigation. The semicircle specimen is chosen to reproduce results similar to the ones by the DLR [11],

although the alternating geometry provides additional stability and removes the need for bonding the specimen to a machined base-plate. The high sine specimen has a nearly identical moment of inertia, and provides insight in the effect of sharper curvature changes on the measured SEA. Lastly, the low sine specimen is supposed to isolate the effect of a lower moment of inertia and more gentle radii on the SEA measurement.

All three specimen shapes are also tested with a reduced section by removing the end-lips and one of the three half-periods. The two half-period sinusoidal shapes are chosen to explore potential dependence of SEA on the number of curvature changes. These have the potential to locally introduce high stress gradients, which in turn can produce greater values of energy absorption.

Two different carbon/epoxy material systems are tested for this study. The so-called 'regular' system is a 250 F-degree cure system with low toughening and intermediate strength fibers. The so-called 'toughened' system is a highly toughened 350 F-degree cure system with higher strength and modulus fibers. The regular and toughened materials feature densities of 1.55 and 1.58 g/cm^3 respectively, which are used for calculating the SEA.

Three different stacking sequences are tested, trying to isolate the effects of longitudinal and shear moduli. The $[0/90]_{3s}$ cross-ply has high axial properties, the $[\pm 45]_{3s}$ angle-ply is characterized by high shear properties, while the $[0/\pm 45]_{2s}$ lay-up has intermediate E_x and G_{xy} values. All specimens have the same nominal thickness of 1.6 mm (0.063 in.) after cure, in order to avoid potential non-linear thickness effects.

A set of specimens that were cured at nominal pressure and temperature but for a period twice as long as the suggested from the manufacturer were tested to isolate the sensitivity of the proposed method to manufacturing errors. Over-curing should result in a more brittle system, which in turn should yield lower SEA values.

Lastly, test speed was varied between 5, 51, and 1524 mm/min (0.2, 2, and 60 in./min) to investigate the ability of the specimen to measure strain-rate sensitivity of the material and lay-up. Although previous work seems to show that dynamic effects become evident only beyond 500–1000 mm/sec (20–40 in./s), it is interesting to verify the validity of measurements in the quasi-static regime at various test speeds.

Results and Discussion

A summary of results is plotted in Table 3, which shows the twenty-four combinations of the parameters that were tested. Only one parameter per configuration is varied. Configurations where all parameters are constant except for the corrugation shape are called families. In Table 3, configurations 1–3 constitute family A. Two repetitions for each configuration were performed, with the exception of configuration 16, which had 4. It should be noted that, although the coefficient of variation (CoV) varies between 0 and 8% for all configuration tested except for the ±45, which requires a separate discussion, further work will need to be performed to build a statistically significant database.

A special discussion needs to be made for the ±45 lay-up, which is characterized by larger variation in measured SEA due to its significantly lower longitudinal modulus. Although macroscopic buckling occurred only in one instance, for configuration 4 featuring the lowest section modulus of all three tested, local buckling of the fronds at the crush front occurred in the other two cases (Figure 16). When it did, it led to significantly decreased SEA, which in turn gave rise to the greater CoV (up to 20%).

Table 3. Summary of results for the configurations tested.

ID	Family	Specimen	Lay-up	Material	No. periods	Repeats	Cure	Left speed (in/min)	Avg SEA (J/g)	CoV
1	A	Low Sine	[0/90]3s	Rejukr	3	2	Regular	2	59	7%
2	A	High Sine	[0/90]3s	Regular	3	2	Regular	2	65	4%
3	A	Semicircle	[0/90]3s	Regular	3	2	Regular	2	70	4%
4	B	Low Sine	[±45]3s	Regular	3	2	Regular	2	19	1%
5	B	High Sine	[±45]3s	Regular	3	2	Regular	2	54	20%
6	B	Semicircle	[±45]3s	Regular	3	2	Regular	2	56	7%
7	C	Low Sine	[0/±45]2s	Regular	3	2	Regular	2	63	3%
8	C	High Sine	[0/±45]2s	Regular	3	2	Regular	2	73	2%
9	C	Semicircle	[0/±45]2s	Regular	3	2	Regular	2	81	5%
10	D	Low Sine	[0/±45]2s	Regular	3	2	Overcured	2	61	1%
11	D	High Sine	[0/±45]2s	Regular	3	2	Overcured	2	67	4%
12	D	Semicircle	[0/±45]2s	Regular	3	2	Overcured	2	71	3%
13	E	Low Sine	[0/90]3s	Tough	3	2	Regular	2	83	7%
14	E	High Sine	[0/90]3s	Tougli	3	4	Regular	2	94	8%
15	E	Semicircle	[0/90]3s	Tough	3	2	Regular	2	93	1%
16	F	Low Sine	[0/90]3s	Tough	2	2	Regular	2	79	1%
17	F	High Sine	[0/90]3s	Tough	2	2	Regular	2	86	7%
18	F	Semicircle	[0/90]3s	Tough	2	2	Regular	2	101	8%
19	G	Low Sine	[0/90]3s	Tough	3	2	Regular	0.2	75	5%
20	G	High Sine	[0/90]3s	Tough	3	2	Regular	0.2	91	1%
21	G	Semicircle	[0/90]3s	Tough	3	2	Regular	0.2	91	4%
22	H	Low Sine	[0/90]3s	Tough	3	2	Regular	60	83	3%
23	H	High Sine	[0/90]3s	Tough	3	2	Regular	60	93	7%
24	H	Semicircle	[0/90]3s	Tough	3	2	Regular	60	98	7%

All other configurations tested achieved stable sustained crushing, with a combination of progressive frond formation and brittle fracturing. In all specimens but the one without the chamfer crushing initiated with load efficiencies near unity, thus suggesting that the simple triggering mechanism is adequate to avoid high spikes in the load trace. The unchamfered specimen reached a crush load efficiency of 2.5, which should be avoided.

The load-stroke trace of configuration 15 is shown in Figure 17, from which the energy absorbed curve can be calculated using Equation (2) and the SEA using Equation (1). The results are normalized to their respective maximum values in order to be plotted in one chart. The EA curve is perfectly linear, and the SEA plot shows also a nearly perfect rectangular step function shape (in a fashion similar to a metallic elastic–perfectly plastic behavior). The same curves are plotted in Figure 18 for configuration 2. The load–deflection curve shows a less ideal behavior, characterized by a shallow trough after the onset of crushing. The change in slope of the nearly linear EA curve, and the increase in SEA during the stroke, possibly due to an increased friction of the long fronds that are being formed, are also visible. The tougher material of configuration 15 absorbed greater energy than configuration 2, and in a more uniform way (Figures 19 and 20). Another kind of less desirable curve is shown in Figure 21, which shows sharper drops in the load trace, and a more defined trough in the SEA curve.

In four of the five families tested, where all parameters are held constant except for the shape of the corrugation, the semi-circular specimen exhibited consistently higher SEA than the high-sine specimen, which in turn yielded higher SEA than the low sine

Figure 16. *Local buckling of the fronds for configuration no. 5.*

specimen (Figure 22). Plotting the measured SEA against the specimen's moment of inertia (I) it seems possible to observe a monotonically increasing trend (Figure 23), with the exception of configuration 4, which buckled prematurely and is not shown. Therefore it appears that the specimens with a larger I will dissipate more energy per unit weight than ones with very similar shape but smaller moment of inertia. With this understanding, which needs to be further supported by more experimental evidence and advanced numerical modeling, all three corrugations offer acceptable crush performance, but yield different SEA measures. This relationship between SEA and section's moment of inertia suggest the possibility of employing a normalized SEA/I value in designing energy-absorbing devices.

It should also be noted that for the same thickness and modulus the semicircle specimen has the highest I, closely followed by the high sine, as mentioned previously. For relatively 'hard lay-ups', or for material systems with high modulus, the buckling load is far greater than the average crush force. However, for 'soft lay-ups' and for lower-performing material forms, such as sheet molding compounds, the buckling load can be lower than the force to initiate and sustain crush, and buckling may occur. This is indeed the case for the $[\pm 45]_{ns}$ lay-up, which buckled for in the low sine specimen but crushed in the other two geometries. This consideration can also be extended to specimens that are tested without trigger, where peak force reaches values that can far exceed sustain crushing, as

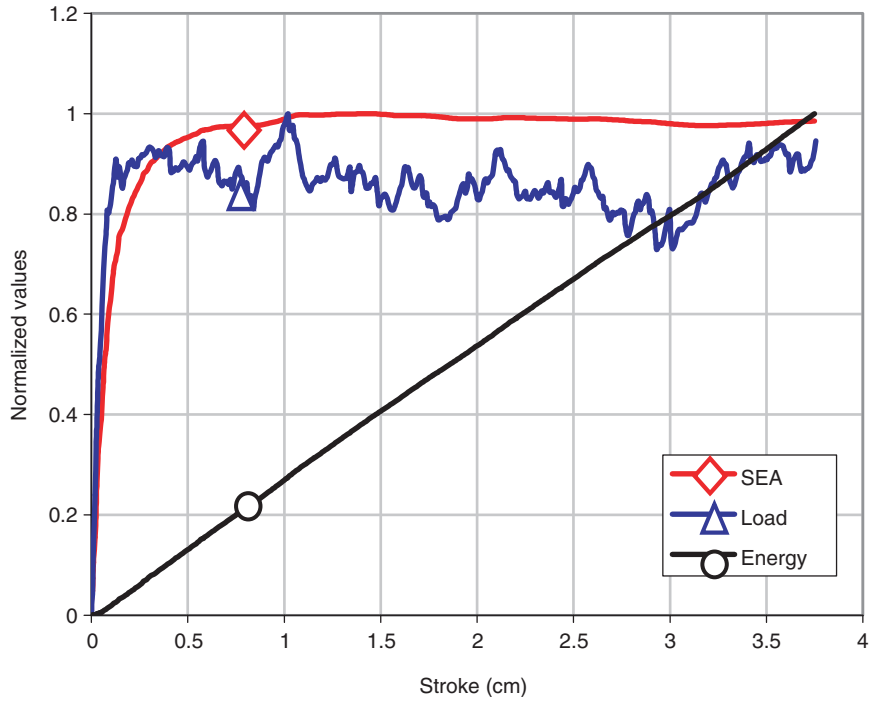

Figure 17. *Plots of normalized load, SEA, and energy absorbed vs. stroke for configuration 15.*

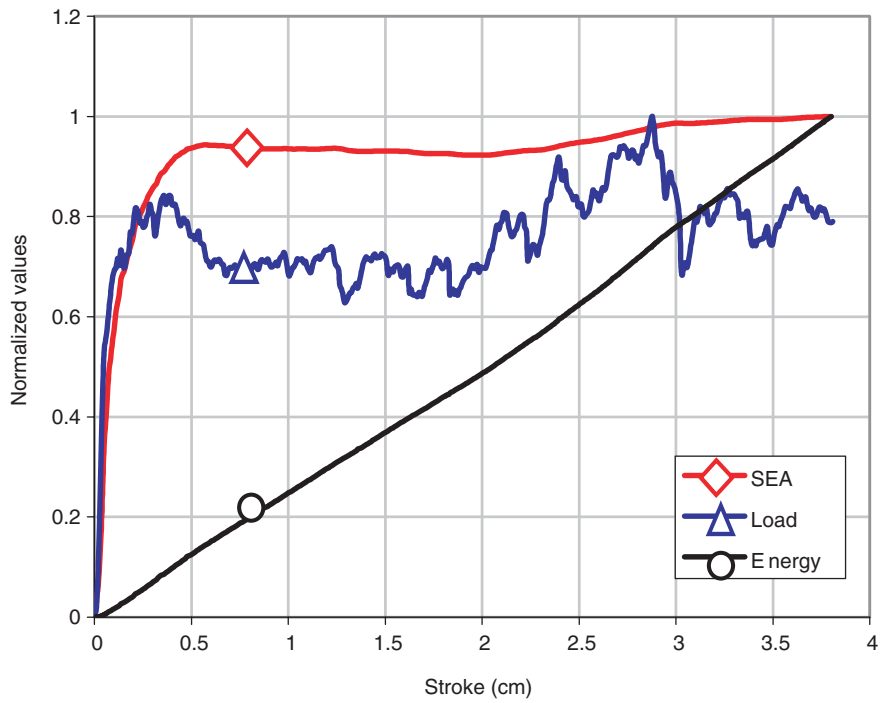

Figure 18. *Plots of normalized load, SEA, and energy absorbed vs. stroke for configuration 2.*

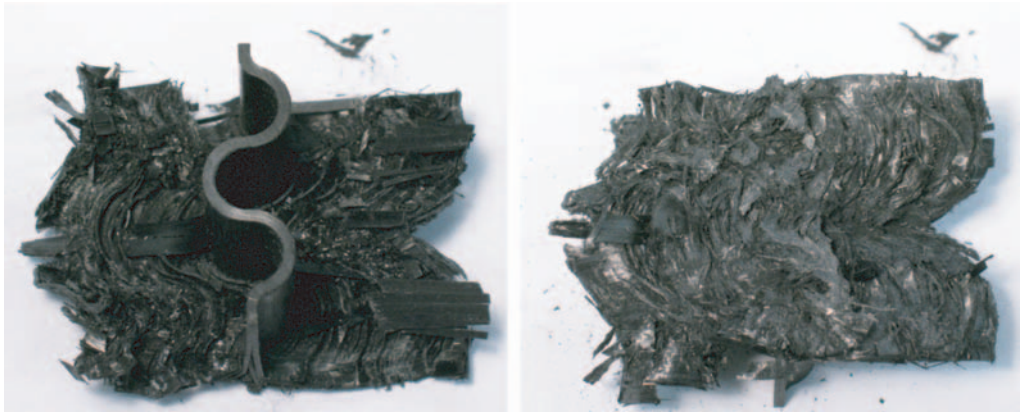

Figure 19. *Top and bottom view of crushed specimen for configuration 15.*

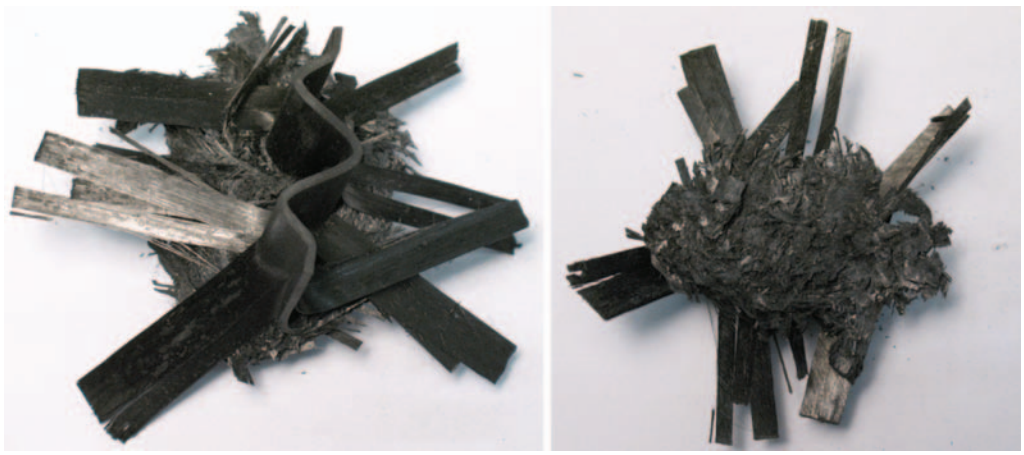

Figure 20. *Top and bottom view of crushed specimen for configuration 2.*

mentioned previously. Therefore, since a possible specimen for test standardization should be capable to be used by the majority of material forms and reinforcement types it is suggested that either the high sine or semicircle specimens are further pursued. The buckling resistance of the web could also be dramatically improved by reducing the length of the specimen to 50.8 mm (2 in.). However, the effective stroke would then be limited severely, as it is suggested to limit the stroke to less than half the specimen length to avoid potential interference of the splayed fronds with the upper moving platen. Shortening the specimen height reduces the effective stroke to less than 25 mm, which could not be adequate to fully capture the crushing behavior of the specimen.

All three corrugated shapes were further machined to remove one of the three half-periods, as well as both end-lips. This attempt to investigate the influence of curvature gradients on the measured SEA shows that such measurement is independent on the number of sinusoid half-periods (Figure 24). This in turn suggests that the corrugation does not create relevant stress concentrations in proximity of the change in curvature. On the other hand, if high stress gradients were present, they would yield increased fracturing

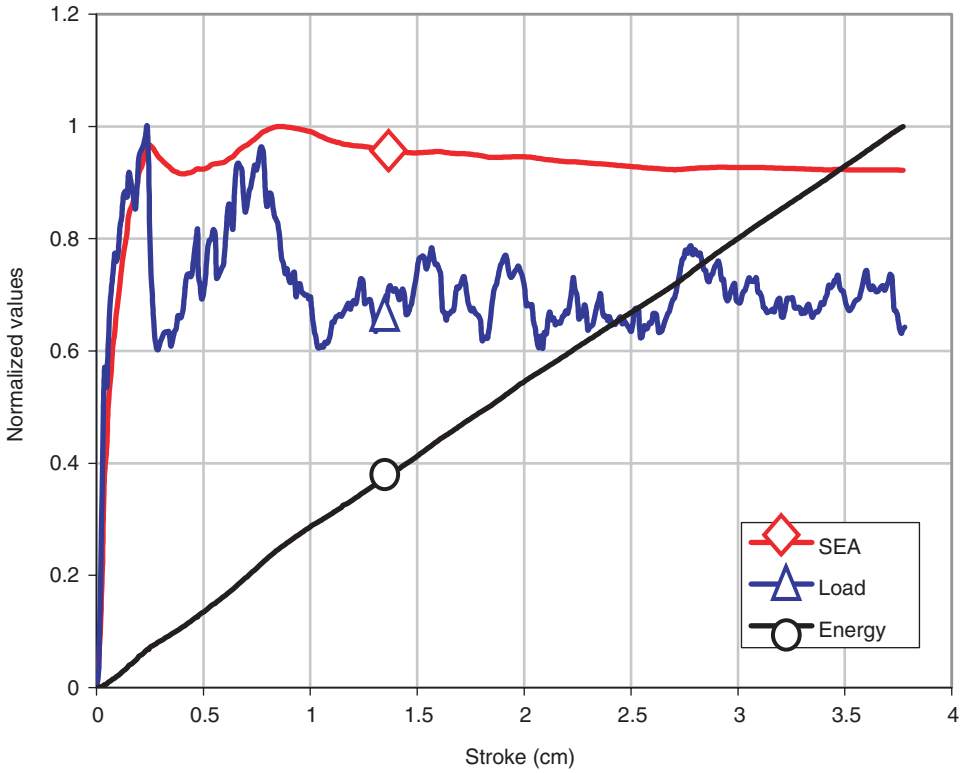

Figure 21. *Plots of normalized load, SEA, and energy absorbed vs. stroke for configuration 1.*

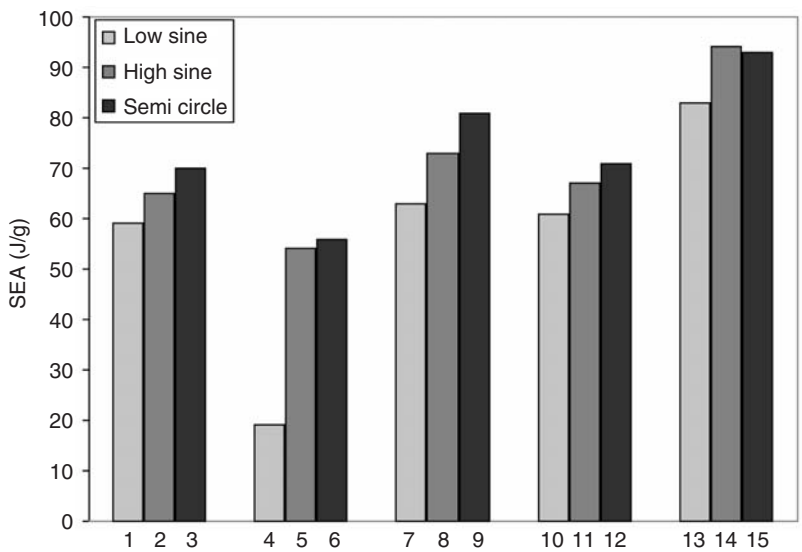

Figure 22. *Comparison of corrugation shape on the measured SEA within families of configurations.*

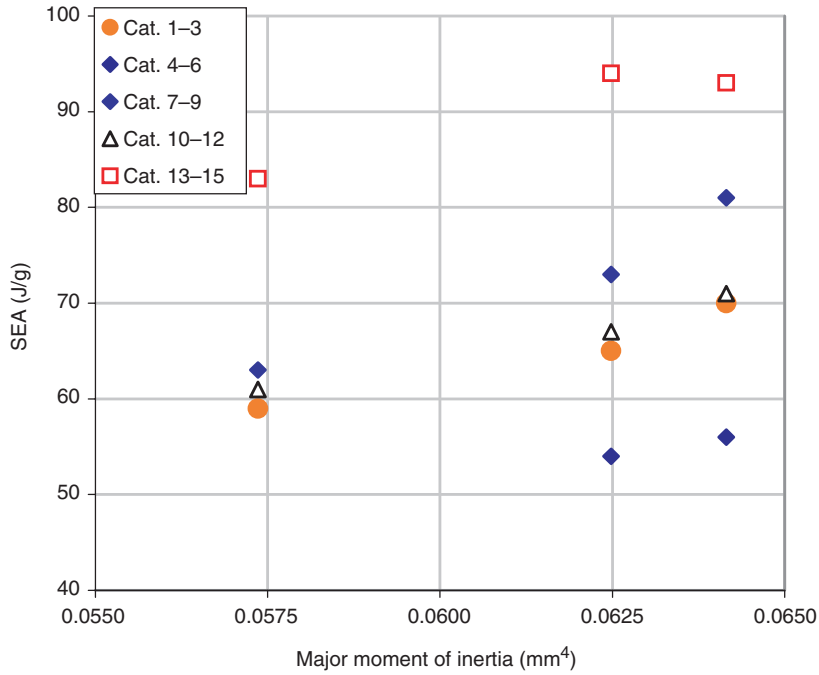

Figure 23. *Measured SEA appears to increase with the section's moment of inertia.*

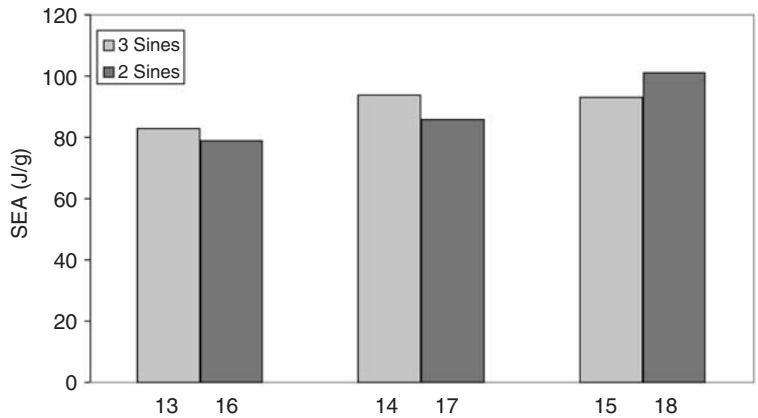

Figure 24. *Sensitivity to number of half-periods for all three specimen shapes.*

and energy dissipation around the radii. In turn, it would suggest that the proposed specimens capture unrealistic (non-natural) failure mechanisms of the material, and hence irrelevant SEA values. With these considerations in mind, the third half-period increases the moment of inertia and hence the buckling resistance of the specimen, and should therefore be employed over a specimen with only one or two half-periods.

The influence of lay-up is investigated in Figure 25 for three families of configurations, and it shows that SEA is not a simple function of neither longitudinal nor shear moduli. For all families tested, $[0/\pm45]_{2s}$ exhibits the highest SEA, closely followed by the $[0/90]_{3s}$.

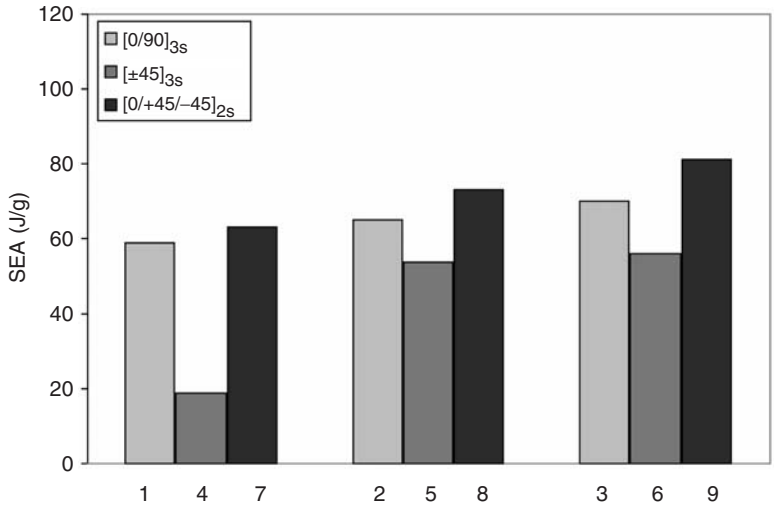

Figure 25. *Variation of SEA with three lay-ups for each corrugation shape.*

The $[\pm 45]_{3s}$ lay-up, even without premature buckling, yields the lowest values of SEA. In general, keeping everything else constant, the SEA increases and decreases both as a function of percent 0 plies and percent 45 plies. With respect to the baseline between the $[0/90]_{3s}$, a slight decrease in axial modulus in exchange for a noticeable increase in shear modulus for the $[0/\pm 45]_{2s}$ yields a higher SEA, while a shear-dominated lay-up such as $[\pm 45]_{3s}$ yields a lower SEA (Figure 26(a) and (b)). Energy absorption confirms to be a complex function of stacking sequence, and further systematic work should be aimed at fully characterizing this behavior.

The effect of varying the material system on the SEA properties is the most dramatic. The highly toughened system, which also features higher modulus and higher strength fibers, clearly shows a greater SEA than the regular system (Figure 27). Similarly, the effect of doubling the curing time in the heated press to introduce voluntarily embrittlement in a test panel shows lower SEA values for all families tested (Figure 28). The different failure modes between tougher and more brittle specimens can also be seen in the preceding Figures 17 and 18.

Test speed was varied between four orders of magnitude (5, 51, and 1524 mm/min) in the quasi-static range. The highly toughened material, designed for crashworthiness applications, as well as applications where damage resistance and tolerance is critical, showed virtually constant SEA measurements. This phenomenon could be attributed to the strain-rate insensitive nature of the material system, although previous observations on tubular specimens appear to exhibit a dynamic threshold in the range of 0.5–1.0 m/s [5,11,18]. Further work would have to be expanded in the dynamic range with the use of a drop tower to further characterize the strain-rate dependence of SEA measurements (Figure 29).

FUTURE WORK

Developing a test method suitable for standardization is a real challenge, mostly because the measured SEA will never represent a true material property, but will inevitably indicate

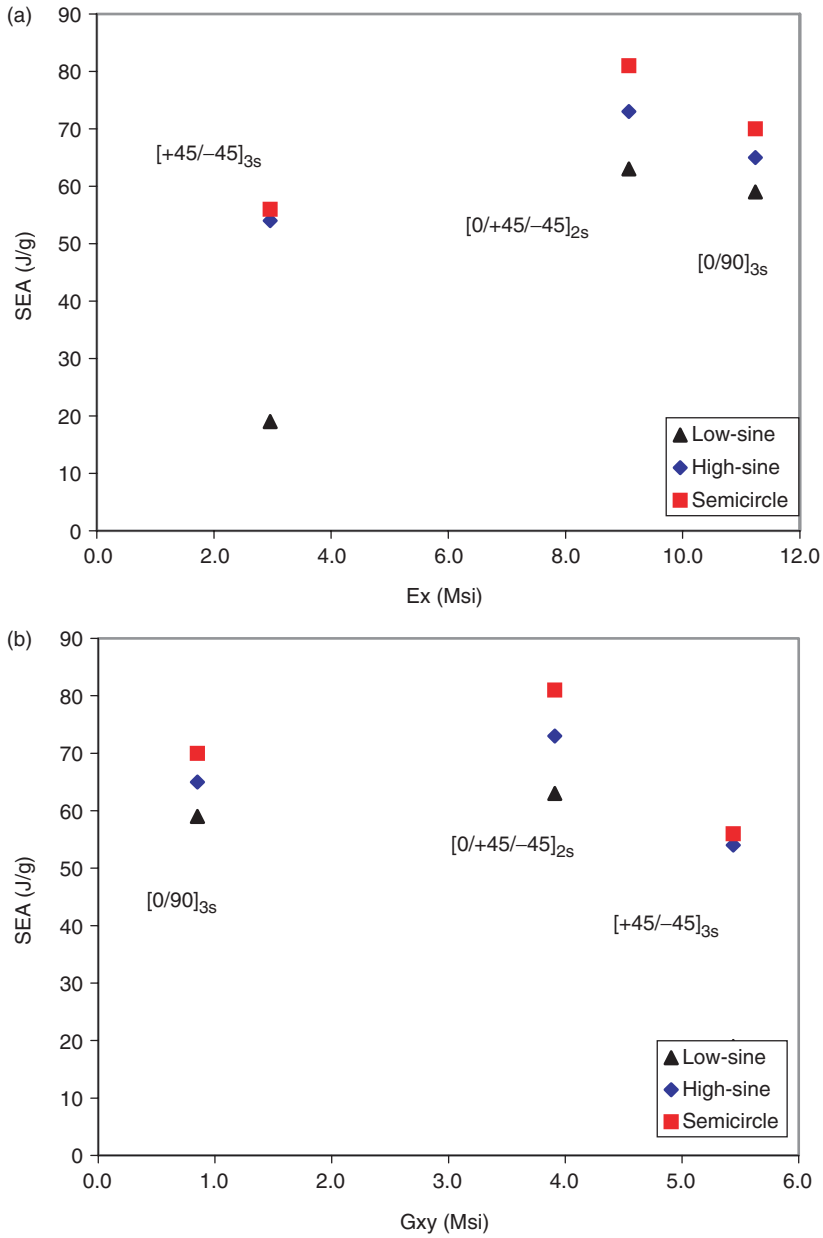

Figure 26. *Variation of SEA with axial (a) and shear (b) moduli.*

a structural property which is uniquely related to the geometry of the specimen used. ASTM D30 Committee on Composite Materials distinguishes between material tests and structural tests, and in the latter fall commonly used tests such as open-hole tension and compression after impact. Variations of geometric characteristics of the test coupons will lead to substantially different results, yet it is important to recognize the relevance of such standards to screen materials and provide design guidelines.

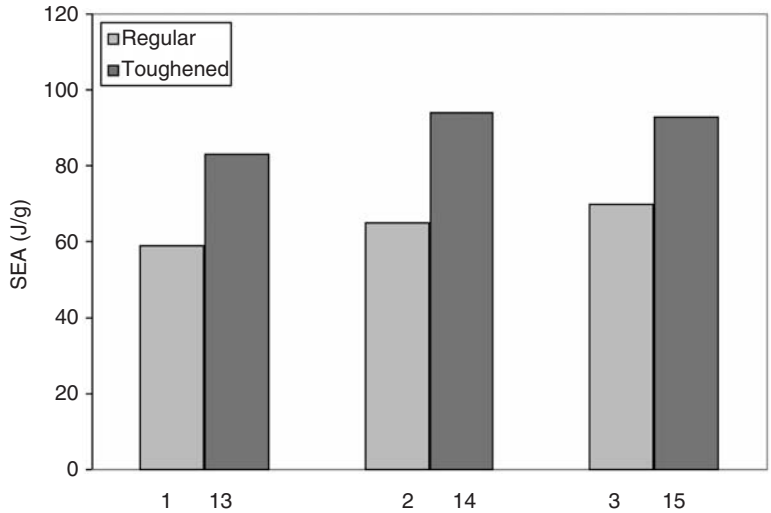

Figure 27. *Specimen's sensitivity to material system (degree of toughening as well as strength and modulus of reinforcement).*

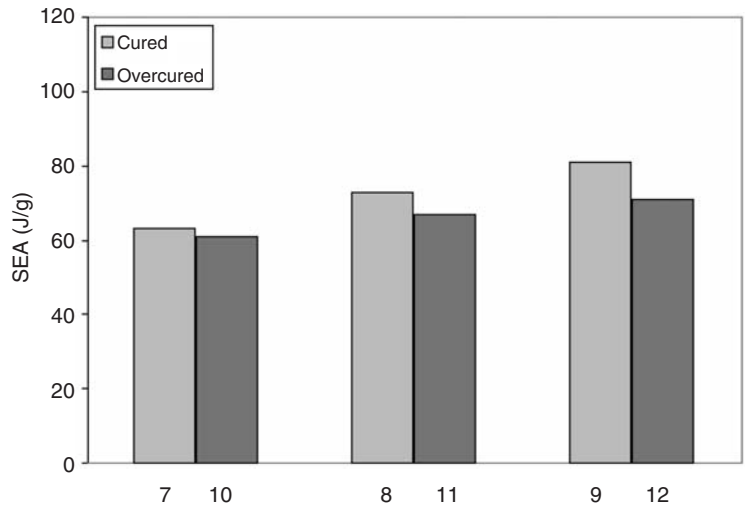

Figure 28. *Specimen's sensitivity to curing errors.*

With this premise, it is imperative that the SEA test standard proposed here yields meaningful and repeatable measurements. To reach such confidence it will be necessary to continue to systematically and carefully characterize the sensitivity of this method to intrinsic as well as test parameters. For example, the influence of specimen length and degree of support (free standing vs. clamped) need to be investigated, as well as the effect of roughness on the crushing surface, and the influence of amplitude of half-periods. The variation of SEA with section's moment of inertia and area needs to be further explored, as it would even suggest revisiting the definition of SEA itself. Previous investigation by Hanagud et al. [24] showed that corrugated web specimens are robust to variations of

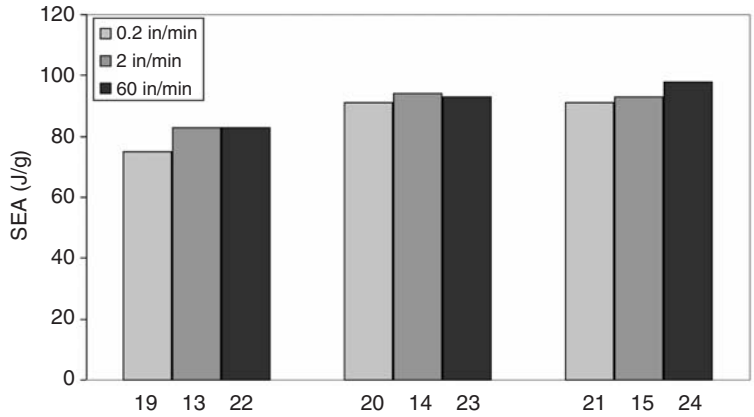

Figure 29. *Variation of SEA with test speed.*

geometric shape parameters such as number of waves (width), degree of corrugation (included angle), and type of trigger mechanism. However, a closer look shows that the trends slightly vary between lay-ups and are likely to vary among materials systems (fiber and resin types) and material forms (fiber architectures). For example, a further look at the effect of depth (or length) of trigger mechanisms is required to understand the associated variation in SEA.

More importantly perhaps, the results obtained with the corrugated specimen will have to be compared with those using a tubular structure (square or circular), a flat specimen with a modified fixture such as that of NASA/ARL, and another relevant self-supporting open section (for example a C-channel). A systematic investigation employing same material systems, forms, lay-ups and manufacturing will provide insight on the validity of the proposed method. At the same time, numerical simulation using explicit dynamic Finite Element codes will be needed to reduce the amount of testing required, expand the range of parametric investigations, and further validate the experimental observations.

CONCLUSIONS

Several aircraft applications employ corrugated webs for dissipating energy during a crash, and many studies have indicated that these shapes offer stable and progressive crushing characteristics. This study proposes the utilization of a corrugated plate specimen as a simple and cost-effective candidate for standardization. Although a limited amount of testing has been performed, preliminary results seem to suggest that the sinusoidal or semicircular geometry is self-stabilizing and requires minimal cost and labor for manufacturing. The investigation conducted has shown that the specimen offers SEA measures that are capable of capturing interesting trends for all intrinsic parameters tested, including sinusoid dimension, material system, and test speed. Maximizing the moment of inertia of the section will enable the testing of material systems with a broad range of properties, hence the high-sine or semicircular specimens appear to be more suitable specimens for standardization than the low sine geometry. Future work needs to determine how these measurements compare with flat and tubular specimens of the same construction, and how these results can be effectively used for design purposes.

ACKNOWLEDGMENTS

The author is the founding chair of the Crashworthiness Working Group of the CMH-17 (Composite Materials Handbook, former MIL-HDBK-17), and would like to thank its active members for their continued support. He also would like to acknowledge Paul Robertson (Aeronautical Test Services) for providing the mold design and manufacturing; Shreeram Raj (Cytec Engineered Materials) and Andrea Dorr (Toray Composites) for donating the prepreg materials; graduate students Francesca Garattoni and Francesco DeLeo for manufacturing the specimens and performing the tests; and the two anonymous reviewers who contributed to the improvement of the paper and the planning of future research activities.

REFERENCES

1. Simula Technologies, A Systems Approach to General Aviation Occupant Protection, NASA Langley Research Center Final Report, TR-00046, June 2000.
2. Carruthers, J.J., Kettle, A.P. and Robinson, A.M. (1998). Energy Absorption Capability and Crashworthiness of Composite Material Structures: A Review, *Applied Mechanics Reviews*, **51**: 635–649.
3. Farley, G.L. and Jones, R.M. (1992). Crushing Characteristics of Continuous Fiber-Reinforced Composite Tubes, *Journal of Composite Materials*, **26**(1): 37–50.
4. Jeryan, R. (2005). Energy Management Working Group Activities, In: *Proceedings of the 48th MIL-HDBK-17 Coordination Meeting – Crashworthiness Working Group*, Charlotte, NC, March 2005.
5. Nailadi, C. (2005). A Summary of the ACC Tube Testing Program, In: *Proceedings of the 49th MIL-HDBK-17 Coordination Meeting – Crashworthiness Working Group*, Santa Monica, CA, December 2005.
6. Jackson, K.E. (2005). Energy Absorption of Composite Materials and Structures, In: *Proceedings of the 49th MIL-HDBK-17 Coordination Meeting – Crashworthiness Working Group*, Santa Monica, CA, December 2005.
7. Bannerman, D.C. and Kindervater, C.M. (1984). Crashworthiness Investigation of Composite Aircraft Subfloor Beam Sections, *Structural Impact and Crashworthiness*, Vol. 2, Conference Papers, Elsevier, London.
8. Wiggenraad, J.F.M. Crashworthiness research at NLR: 1990–2003, NLR TP-2003–217, June 2003.
9. McCarthy, M.A., Harte, G.A., Wiggenraad, J.F.M., Michielsen, A.L.P.J., Kohlgrueber, D. and Kamoulakos, A. (2006). Finite Element Modeling of Crash Response of Composite Aerospace Sub-Floor Structures, *Computational Mechanics*, **26**: 250–258.
10. *Composite Materials Handbook (CMH-17)*, Volume 3, Chapter 13, Rev. G.
11. Johnson, A. (2006). Determination of Composite Energy Absorption Properties, In: *Proceedings of the 50th MIL-HDBK-17 Coordination Meeting – Crashworthiness Working Group*, Chicago, IL, July 2006.
12. Bolukbasi, A.O. and Laananen, D.H. (1995). Energy Absorption in Composite Stiffeners, *Composites*, **26**(4): 291–301.
13. Lavoie, J.A. and Morton, J. (1993). Design and Application of a Quasistatic Crush Test Fixture for Investigating Scale Effects in Energy Absorbing Composite Plates, NASA CR 4526, July 1993.
14. Jackson, K., Morton, J., Lavoie, J. and Boitnott, R. (1994). Scaling of Energy Absorbing Composite Plates, *Journal of the AHS*, **39**(1): 17–23.
15. Lavoie, J.A. and Kellas, S. (1996). Dynamic Crush Tests of Energy-Absorbing Laminated Composite Plates, *Composites Part A*, **27**(6): 467–475.

16. Daniel, L., Hogg, P.J. and Curtis, P.T. (1999). The Relative Effects of Through-Thickness Properties and Fibre Orientation on Energy Absorption by Continuous Fibre Composites, *Composites Part B*, **30**: 257–266.
17. Cauchi Savona, S. and Hogg, P.J. (2006). Investigation of Plate Geometry on the Crushing of Flat Composite Plates, *Composites Science and Technology*, **66**(11–12): 1639–1650.
18. Barnes, G. (2005). Composite Crush Coupon Testing, In: *Proceedings of the 49th MIL-HDBK-17 Coordination Meeting – Crashworthiness Working Group*, Santa Monica, CA, December 2005.
19. Jacob, G.C., Fellers, J.F., Simunovic, S. and Starbuck, J.M. (2002). Energy Absorption in Polymer Composites for Automotive Crashworthiness, *Journal of Composite Materials*, **36**(7): 813–850.
20. Jacob, G.C., Fellers, J.F., Starbuck, J.M. and Simunovic, S. (2004). Crashworthiness of Automotive Composite Material Systems, *Journal of Applied Polymer Science*, **92**: 3218–3225.
21. Brimhall, T.J. (2006). Measurement of Static and Dynamic Friction Energy Absorption in Carbon/Vinyl Ester Composite, In: *Proceedings of the 6th SPE Automotive Composites Conference*, Troy, MI, September 2006.
22. Dormegnie, D., Coutellier, D., Delsart, D. and Deletombe, E. (2003). Studies of Scale Effects for Crash on Laminated Structures, *Applied Composite Materials*, **10**: 49–61.
23. Fleming, D.C. and Nicot, F. (2003). Crushing of Flat Graphite/Epoxy Laminates Using a Column Specimen, *Journal of Composite Materials*, **37**(24): 2225–2239.
24. Hanagud, S., Craig, I., Sriram, P. and Zhou, W. (1989). Energy Absorption Behaviour of Graphite Epoxy Composite Sine Webs, *Journal of Composite Materials*, **23**(5): 448–459.
25. Feraboli, P. Current Efforts in Standardization of Composite Materials Testing for Crashworthiness and Energy Absorption – Feraboli, P. – *47th AIAA/ASME/ASCE/AHS/ ASC Structures, Dynamics and Materials Conference*, No. 2006–2217, Newport, RI, May 2006.
26. San Vicente, J.L., Beltrán, F. and Martínez, F. Simulation of Impact on Composite Fuselage Structures, *European Congress on Computational Methods in Applied Sciences and Engineering, ECCOMAS 2000*, Barcelona, Spain, September 2000.
27. Jackson, K.E., Fasanella, E.L., Boitnott, R.L. and Lyle, K.H. (2003). Full-Scale Crash Test and Finite Element Simulation of a Composite Prototype Helicopter, NASA TP-2003–212641, ARL-TR-2824, August.